mathematics

MDPI

Article

Economic Load Dispatch Problem Analysis Based on Modified Moth Flame Optimizer (MMFO) Considering Emission and Wind Power

Hani Albalawi [1,2], Abdul Wadood [1,2,*] and Herie Park [3,*]

[1] Renewable Energy and Environmental Technology Center, University of Tabuk, Tabuk 47913, Saudi Arabia; halbala@ut.edu.sa
[2] Electrical Engineering Department, Faculty of Engineering, University of Tabuk, Tabuk 47913, Saudi Arabia
[3] Department of Electrical Engineering, Dong-A University, Busan 49315, Republic of Korea
* Correspondence: wadood@ut.edu.sa (A.W.); bakery@donga.ac.kr (H.P.)

Abstract: In electrical power system engineering, the economic load dispatch (ELD) problem is a critical issue for fuel cost minimization. This ELD problem is often characterized by non-convexity and subject to multiple constraints. These constraints include valve-point loading effects (VPLEs), generator limits, emissions, and wind power integration. In this study, both emission constraints and wind power are incorporated into the ELD problem formulation, with the influence of wind power quantified using the incomplete gamma function (IGF). This study proposes a novel metaheuristic algorithm, the modified moth flame optimization (MMFO), which improves the traditional moth flame optimization (MFO) algorithm through an innovative flame selection process and adaptive adjustment of the spiral length. MMFO is a population-based technique that leverages the intelligent behavior of flames to effectively search for the global optimum, making it particularly suited for solving the ELD problem. To demonstrate the efficacy of MMFO in addressing the ELD problem, the algorithm is applied to four well-known test systems. Results show that MMFO outperforms other methods in terms of solution quality, speed, minimum fuel cost, and convergence rate. Furthermore, statistical analysis validates the reliability, robustness, and consistency of the proposed optimizer, as evidenced by the consistently low fitness values across iterations.

Keywords: economic load dispatch; wind power; emission; nature-inspired optimization; modified technique; moth flame optimizer

MSC: 68T20

Citation: Albalawi, H.; Wadood, A.; Park, H. Economic Load Dispatch Problem Analysis Based on Modified Moth Flame Optimizer (MMFO) Considering Emission and Wind Power. *Mathematics* **2024**, *12*, 3326. https://doi.org/10.3390/math12213326

Academic Editors: Yuan Cao, Chunsheng Wang and Liqing Liao

Received: 21 September 2024
Revised: 20 October 2024
Accepted: 22 October 2024
Published: 23 October 2024

1. Introduction

Growing power demand has significantly increased the generation costs. Hence, there is an increasing need to economically disengage the power in order to reduce fuel expenses and ensure the consistent functioning of the power grid [1,2]. To minimize fuel costs and adhere to all system and producing unit constraints, the economic load dispatch (ELD) problem primarily seeks to organize the output of power generation units to meet the needed load demand in a logical manner. Newton–Raphson, lambda iteration, dynamic programming, and gradient methods are some of the well-established procedures that have been suggested in the literature as appropriate ways to address this particular issue. However, as shown in [3], the gradient approach demonstrates a sluggish rate of convergence and has difficulties when faced with constraints related to inequality. The convergence characteristics of Newton's approach are subject to the influence of the initial estimation, which might potentially hinder its effectiveness in obtaining an optimal solution if the initialization is wrong. The linear programming approach is plagued by inaccuracies and the approximation of piece-wise linear costs. Additionally, as mentioned in [3], the

application of quadratic programming to the piece-wise quadratic cost approximation demonstrates inefficiency if the step size is not appropriately chosen. The interior point approach, although commonly seen as more computationally efficient, may not yield a realistic solution for non-linear objective functions [4]. Furthermore, it is important to acknowledge that these traditional approaches need the utilization of incremental fuel cost curves, which demonstrate a consistent upward trend or incremental linear trend. The ELD problem demonstrates input–output features that are non-convex, non-linear, and non-smooth [5]. In order to get beyond the limitations of conventional methods, several soft computing approaches have been proposed in the literature.

In [5], an innovative methodology for oppositional pigeon-inspired optimization has been proposed to address the prevalent problem of premature convergence in the case of power system problem optimization. A chameleon swarm algorithm is proposed in [6] to address the ELD problem. In addition, a comprehensive exploitation phase is carried out to tackle the problem of ELD using quasi-quadratic programming for smart building [7]. In [8], a Q-learning-based search optimization was used to solve the ELD problem for different IEEE benchmark functions. The ELD problem is solved as multi-objective economic load dispatch (MELD) considering generation cost and transmission losses in [9] using the Particle Swarm Optimization (PSO) algorithm. In [10], the modified version of PSO was used for the utilization of adaptive acceleration constants. This strategy helps in determining the most suitable value for the acceleration constant in the evaluation of fitness function values. In [11], a hybrid approach was utilized consisting of bacteria foraging (BSA) and PSO to deal with the non-convex ELD problem considering the influence of valve-point effects. This inclusion aims to decrease the degree of unpredictability in the search procedure and improve the collective behavior of the optimizer. The ELD problem has been solved utilizing the application of invasive weed optimization [12] while considering the effects of valve-point loading effect and prohibited operation zones. In order to best solve the ELD problem, grey wolf optimizer (GWO) has been used for different IEEE test systems [13]. In [14], an ant lion optimizer was recalled to solve the ELD problem on four compact test systems keeping in view the valve-point effect scenario. A novel hybrid methodology was designed in [15] by combining the PSO with pattern search to solve the ELD problem formulation. In [16], a combination of the Big Bang–Big Crunch (BB-BC) and PSO optimization techniques has been suggested for solving the ELD problem in a more resilient and efficient way. Artificial bee colony (ABC) optimization has been utilized in [17] to solve the ELD problem considering the valve-point effects for different IEEE test systems, i.e., IEEE three, thirteen, and forty systems.

In [18], the authors explore the possibility of improving the ELD problem solution by the deployment of a hybrid algorithm that combines a genetic algorithm (GA) and differential evolution (DE) with a dynamically coordinated PS algorithm considering the valve-point loading effect. In order to best solve the ELD problem including the valve-point effects, a new variant of PSO known as catfish PSO has been utilized in [19]. In [20], the authors examined the conventional ELD problem and proposed a novel approach that involves the elimination of inefficient generators through the utilization of the differential evolution (DE) technique. The implementation of this methodology has resulted in a reduction of 19.88% in the overall fuel cost in comparison to conventional methods. In [21], a comparative analysis of five soft computing approaches, specifically DE, PSO, evolutionary programming (EP), genetic algorithm (GA), and simulated annealing (SA), has been utilized to solve the dynamic ELD problem. This comparative analysis takes into account several constraints, including limitations on the generator ramp rate. In [22], an improved version of teaching–learning-based optimization with incorporation of quasi-oppositional-based learning has been proposed to enhance the exploration and convergence characteristics of the proposed optimizer in order to best solve the ELD problem. To tackle the ELD problem, a modified version of the DE approach is suggested in [23]. The proposed optimizer entails the incorporation of a tournage-best vector during the mutation phase.

The generation of electrical energy from fossil fuel-based thermal power stations has led to an increase in the emission of harmful pollutants, including oxides of nitrogen (NOx), sulfur oxides (SO), and carbon monoxide (CO). To address these environmental issues, computational methods have been developed to optimize power generating efficiency while reducing hazardous emissions. The integration of renewable energy sources (RESs), such as wind and solar power, has significantly alleviated the challenges related to rising generating prices and harmful fossil emissions [23]. The assimilation of energy from RESs into thermal power systems has necessitated alterations to the traditional quadratic equation utilized for calculating the cost of fuel. These enhancements include the incorporation of Beta and Weibull distribution functions, which account for the probabilistic fluctuations in the supply of solar and wind energy [24], respectively. PSO is a global methodology inspired by metaheuristic principles used to achieve optimal results in ELD integrated with wind power for the development of hybrid energy generating systems [25]. The enhancement of wind power availability, in conjunction with thermal power generation units, has been accomplished by a unique optimization technique known as HIC-SQP [26]. The aim is to optimize direct costs, inflated costs, and underestimated costs to reduce both power generating expenses and hazardous gas emissions. In [27], an exchange market algorithm (EMA) has been recalled to solve the ELD problem with wind power integration.

The optimization of the ELD problem is crucial for effective power grid management due to rising global energy demands and power generation costs as well as with integration of renewable energies Conventional approaches have difficulties with restrictions and non-convexity in ELD to handle the inherent unpredictability and non-linear dynamics resulting in unsatisfactory solutions The aforementioned research indicates that a majority of the techniques [5–25] require the adjustment of a significant amount of control parameters. Therefore, in order to obtain an optimal solution, it is necessary to accurately adjust the control settings, a process that can be both time-consuming and laborious. The moth flame optimization (MFO) algorithm [28] is a recently developed methodology that draws inspiration from the migration patterns of moths in relation to moonlight. The moth employs a mechanism called transverse orientation to enhance its movement [29]. This technique has demonstrated rapid convergence and effective utilization in tackling diverse engineering design issues. However, in the conventional MFO approach, in the last step of iterative optimization, the majority of individuals are concentrated in a limited terrestrial area surrounding the present ideal individual [30–33]. If sophisticated multimodal global optimization problems are being addressed, it is possible for the entire population to quickly achieve the local optimum [31] and be prone to early convergence.

This paper proposes the modified version of MFO known as MMFO. The MMFO technique entails incorporating the idea of the Archimedean spiral into the conventional MFO; employing these modifications has led to improvements in the resilience, precision, and search efficiency of the optimizer while also drastically lowering the number of iterations needed to obtain the best solution. This Archimedean spiral enables moths to perform adaptive movements, which ensures a balanced exploration of the search space early in the optimization process and a more focused exploitation near the optimal solutions in later stages. This study presents the MMFO methodology as a potential resolution for the ELD problem.

The key contribution of this paper is expressed as follows:

1. A novel metaheuristic optimization algorithm referred to as MMFO that aims to improve the exploration capacity of the traditional MFO to the ELD problem.
2. The proposed MMFO is successfully applied to four well-known IEEE ELD test systems as well as on 11 benchmark functions to verify the MMFO.
3. The proposed approach is validated in independent runs using various statistical illustrations, including minimal fitness value quantile plots, boxplots, histograms, standard normal plots, and cumulative distribution function plots for each distinct case study for accuracy, robustness, and stability.

The subsequent sections of this paper are organized in the following manner. The problem formulation of the ELD problem is presented in Section 2. The methods for solving the problem are elaborated in Section 3. The findings and subsequent statistical analysis are discussed in Sections 4 and 5.

2. Mathematical Modeling of Problem Formulation

The ELD problem is an optimization problem with constraints that seeks to streamline the allocation of total power to different generating units by optimizing the overall fuel and emission costs. Within the framework of the ELD problem, specific limitations are considered, including the equilibrium of power in the presence and absence of transmission line losses, the maximum capacity for production, and the influence of valve-point loading [22].

2.1. Objective Function

Minimizing the overall amount of fuel used and the amount of pollution from power plants is the main goal of the ELD problem. Therefore, as shown below, the objective function is created by adding the fuel prices of individual dedicated generating units and the emissions from fossil-fueled thermal units, weighted by their respective contributions.

$$F_1 = \sum_{i=1}^{N} C_i(P_i) + \sigma \times \sum_{i=1}^{N} E_i(P_i) \quad (1)$$

For the sake of this discussion, we will use the notation $E_i(P_i)$ to indicate emissions, $C_i(P_i)$ to indicate fuel cost, N to denote the number of generating units, and P_i to indicate active power generated by the i-th generating unit, while σ denotes $C(p_i)^{max}$ and $E(p_i)^{min}$.

2.1.1. Characteristics of a Smooth Cost Function

The quadratic function is used to express the smooth fuel cost characteristic function in the standard ELD problem, as explained in reference [22].

$$\sum_{i=1}^{N} C_i(P_i) = \sum_{i=1}^{N} a_i + b_i P_i + c_i P_i^2 \quad (2)$$

The coefficients representing the fuel cost of the i-th unit are represented by a_i, b_i, and c_i.

2.1.2. Characteristics of Non-Smooth Cost Functions

The output power of the generating unit is regulated via several valves in thermal power plants. Incoming steam flow is mostly controlled by these valves. Thus, the steam valves are opened in response to rising power demand, which causes a spike in losses and changes in the cost curve's shape. The effect that has been described is sometimes called a valve-point loading effect. Considering the numerous non-differential scores and non-smooth features in the cost curve, this phenomenon of valve-point loading [22] is important. Here, we show how the existence of valve-point effects transforms the objective function of the ELD problem into a non-convex quadratic and sinusoidal function.

$$F_2 = \sum_{i=1}^{N} C_i(P_i) = \sum_{i=1}^{N} a_i + b_i P_i + c_i P_i^2 + |e_i sin\left(f_i\left(P_i^{min} - P_i\right)\right)| \quad (3)$$

The cost coefficients, denoted as e_i and f_i, are used to illustrate the effects of valve-point loading. Additionally, $P_i{}^{min}$ is employed to show the minimal active power generation limit of the i-th generator.

2.1.3. Characteristics of Non-Smooth Emission Functions

Fossil fuel generating units are primarily responsible for emitting two main pollutants, namely SOx and NOx. The mathematical expression that represents the functionality of the overall pollutant emissions is as follows.

$$\sum_{i=1}^{N} E_i(P_i) = \sum_{i=1}^{N} \alpha_i + \beta_i P_i + \gamma_i P_i^2 + \eta_i \exp(\delta_i P_i) \tag{4}$$

The emission coefficients of the i-th generator are denoted by α_i, β_i, γ_i, η_i, and δ_i. The equation presented above demonstrates that the pollutant emission function has a high degree of non-linearity, mostly attributed to the inclusion of both quadratic and exponential terms.

2.1.4. Wind Power Generation Availability Cost Function

A significant advantage in electrical power generation with regard to cost-effectiveness and environmental sustainability is the incorporation of wind power into thermal power producing units. Several models aim to explain the scheduling of operational generating cost and real power generation in power generation systems that include both wind and thermal power units. Given the unpredictable nature of wind speed, the power generation operator is unsure about the availability of wind power. Given the discrepancy between the actual and predicted power output, it is possible that there was an overestimation of the wind power availability. This could have resulted in the need to purchase additional electricity to meet the load requirements. Occasionally, there may be surplus power resulting from underestimating the availability of wind power. This surplus power is then utilized to compensate the wind power suppliers for the costs incurred from underutilizing all of the available wind power. The following model can be used to show the total cost of generating wind electricity [33].

$$C_3 = \sum_{n=1}^{wg} \left[\left(C_{W.P(DIR,n)} + C_{W.P(OE,n)} \right) + C_{W.P(UE,n)} \right] \tag{5}$$

The entire number of wind power generating units is denoted by wg, and the variable C_3 stands for the aggregate cost of wind power generation. Here, $C_{W.P(DIR,n)}$ refers to the direct cost, $C_{W.P(OE,n)}$ to the overestimated cost, and $C_{W.P(UE,n)}$ to the underestimated cost as they relate to wind power generating units. A direct proportionality exists between CW and the output of wind power generation. In terms of mathematics, the nth wind power generating unit can be expressed as P (DIR, n).

$$C_{W.P(DIR,n)} = \sum_{n=1}^{wg} (q_n \times W.P_n) \tag{6}$$

The coefficient qn in Equation (6) represents the direct electrical energy cost from the nth wind power generating unit, measured in dollars per megawatt-hour (MWh). On the other hand, W represents the true electrical output power, measured in megawatts (MW), from the nth wind power producing unit. The variable C_W represents the unbalanced overestimated cost resulting from an overestimation of wind power availability. In response to a lack of electrical power from wind power generating units, more real power in megawatts (MW) is obtained. This can be mathematically represented as follows:

$$C_{W.P(OE,n)} = \sum_{n=1}^{wg} (C_{rw,n} \times X(V_{oe,n})) \tag{7}$$

The cost coefficient for overestimation for each wind power generating unit is represented by $C_{rw,n}$ and is measured in dollars per megawatt-hour (MWh), whereas $X(V_{OE,n})$

represents the predicted value of wind power overestimation for the nth wind power generating unit, as demonstrated in Equation (8).

$$X(V_{OE,n}) = W.P_n\left[\ 1-\exp\left(-\frac{V_{IN,n}^{K_n}}{C_n^{K_n}}\right)+\exp\left(-\frac{V_{OUT,n}^{K_n}}{C_n^{K_n}}\right)\ \right]+\left(\ \frac{W.P_{r,n}\times V_{IN,n}}{V_{r,n}-V_{IN,n}}+W.P_n\ \right).\left[\ \exp\left(-\frac{V_{IN,n}^{K_n}}{C_n^{K_n}}\right)-\exp\left(-\frac{V_{1,n}^{K_n}}{c_n^{km}}\right)\ \right]+ \left(\frac{W.P_{r,n}\times C_n}{V_{r,n}-V_{IN,n}}\right)\left\{\ \Gamma\left[1+\frac{1}{K_n},\left(\frac{V_{1,n}}{c_n}\right)^{K_n}\right]-\Gamma\left[1+\frac{1}{K_n},\left(\frac{V_{IN,n}}{C_n}\right)^{K_n}\right]\ \right\} \tag{8}$$

The cut-in, cut-out, and rated wind speeds are represented by the variables V_{IN}, V_{OUT}, and Vr, respectively, and are expressed in meters per second. One way to represent the intermediary parameter is as $V_1 = V_{IN} + (Vr - V_{IN}) \times W.P_1/W.Pr$. The coefficients C_n and K_n represent the size and shape factor, respectively, for the nth wind power generating unit in the Weibull distribution. In megawatts (MW), $W.Pn$ and $W.Pr$ denote the electrical power produced and rated for the nth wind power producing unit, respectively. Additionally, the following mathematical expression can be used to describe the gamma function, which is defined by its incompleteness and limited parameter count of two [33].

$$\Gamma(p,c) = 1/\Gamma(c) \times \int_0^p t^{c-1}e^{-t}dt \tag{9}$$

A typical gamma function consists of a solitary parameter that is expressed as follows:

$$\Gamma(p) = \int_0^p t^{p-1}e^{-p}dt \tag{10}$$

The penalty cost, denoted as $C_{W.P(UE,n)}$, arises from the underestimation of wind power availability, wherein the actual active power generated by wind power producing units exceeds the forecast active power. Compensation is offered to cover the costs incurred by wind power suppliers in this context.

$$C_{W.P(UE,n)} = \sum_{n=1}^{wg}\left(C_{ew,n} \times Y(V_{UE,n})\right) \tag{11}$$

$C_{ew,n}$ represents the cost coefficient for underestimate in dollars per megawatt-hour (MWh) for the nth wind power producing unit. Equation (12) mathematically represents the expected value of wind power underestimate for the nth wind power producing unit, denoted as $Y_{(VUE,n)}$.

$$Y(V_{UE,n}) = (W.P_{r,n} - W.P_n)\left[\ \exp\left(-\frac{V_{r,n}^{K_n}}{C_n^{K_n}}\right)-\exp\left(-\frac{V_{OUT,n}^{K_n}}{C_n^{K_n}}\right)\ \right]+\left(\ \frac{W.P_{1,n}\times V_{IN,n}}{V_{r,n}-V_{IN,n}}+W.P_n\ \right).\left[\ \exp\left(-\frac{V_{r,n}^{K_n}}{C_n^{K_n}}\right)-\exp\left(-\frac{V_{1,n}^{K_n}}{c_n^{kn}}\right)\ \right]+ \left(\frac{W.P_{r,n}\times C_n}{V_{r,n}-V_{IN,n}}\right)\left\{\ \Gamma\left[1+\frac{1}{K_n},\left(\frac{V_{1,n}}{c_n}\right)^{K_n}\right]-\Gamma\left[1+\frac{1}{K_n},\left(\frac{V_{r,n}}{C_n}\right)^{K_n}\right]\ \right\} \tag{12}$$

To model the objective function, one can combine the quadratic fuel cost function, which includes V.P.L.E (Equation (3)), with the wind power generation availability cost function (Equation (5)). This combination results in the total generating cost (*TGC*) in dollars per hour:

$$TGC = \sum_{m=1}^{tg}\left[\ \begin{array}{l} A_m + B_mP_m + C_mP_m^2 + \\ abs(E_m \sin(F_m(P_{m,\min} - P_m))) \end{array}\ \right] + \sum_{n=1}^{wg}\left[\ \begin{array}{l} (q_n \times W.P_n) + (C_{rw,n} \times X(V_{oe,n}) + \\ (C_{ew,n} \times Y(V_{UE,n}) \end{array}\ \right] \tag{13}$$

2.2. Constraint Functions

2.2.1. Constraint on Power Balance

As stated in reference [22], it is expected that the aggregate power produced by dedicated generators will be equal to the combined value of the load demand (PD) and the entire losses incurred during transmission.

$$\sum_{i=1}^{N} P_i - P_D - P_L = 0 \tag{14}$$

The symbol P_L represents the overall transmission loss, and P_D is the load demand. The calculation of losses associated with the transmission of electricity from the producing station to the load is often performed by load flow analysis or by utilizing Kron's loss coefficients, as outlined below.

$$P_L = \sum_{i=1}^{N}\sum_{j=1}^{N} P_i B_{ij} P_j + \sum_{i=1}^{N} P_i B_{0i} + B_{00} \tag{15}$$

The variables B_{ij}, B_{0i}, and B_{00} represent the loss B coefficients and constants under typical operational circumstances.

2.2.2. Constraints on Generation Limits

The maximum Pmax and minimum Pmin restrictions, as indicated in reference [22], and the active power-generated output of each producing unit must meet the specified requirements.

$$P_i^{min} \le P_i \le P_i^{max}, f \text{ or } i = 1, 2, 3, \ldots, N. \tag{16}$$

2.2.3. Ramp Rate Limit Constraints

The power outputs of thermal power units are limited by the ramp rate restrictions due to their inertia. This limitation is beneficial for prolonging the service life of the units and is characterized as follows:

$$\begin{cases} P_{t,i} - P_{t-1,i} \le UR_i \\ P_{t-1,i} - P_{t,i} \le DR_i \end{cases} \tag{17}$$

3. Design Methodology Using MMFO

3.1. Moth Flame Optimization

A new swarm intelligence optimization technique called the moth flame optimization (MFO) algorithm was introduced by Seyedali Mirjalili in 2015 [28]. It takes its cue from the nighttime spiral flight of a moth, which changes its direction of flight in response to the moon. However, in the case of artificial flame which is very close as compared to the moon, moths would eventually form a spiral flight path toward the flame, keeping their angle with the artificial light constant. The MFO is capable of exploring many solution spaces and has excellent parallel optimization abilities. For multimodal and non-convex problems where there is the possibility of many local optimum points, the MFO is more suitable.

3.1.1. Initialize Parameters

The MFO is fundamentally a swarm intelligence optimization algorithm. In the ELD problem, the candidate solutions are represented by m, where m refers to the moths. Moths navigate either in a one-dimensional or multi-dimensional space within the feasible domain,

with their flight paths defining the range of possible solutions. The population of moths, M, is described as follows:

$$M = \begin{bmatrix} m_{1,1} & m_{1,2} & \cdots & m_{1,d} \\ m_{2,1} & m_{2,2} & \cdots & m_{2,d} \\ \vdots & \vdots & \ddots & \vdots \\ m_{n,1} & m_{n,2} & \cdots & m_{n,d} \end{bmatrix} \tag{18}$$

Here, d is dimension size, where n represent the number of moths.

Every moth in the MFO has a matching flame, and the moth updates its position by flying along the flame. The flame that the dimension represents as F is matched by the moth. The flame's position is stated as follows:

$$F = \begin{bmatrix} F_{1,1} & F_{1,2} & \cdots & F_{1,d} \\ F_{2,1} & F_{2,2} & \cdots & F_{2,d} \\ \vdots & \vdots & \ddots & \vdots \\ F_{n,1} & F_{n,2} & \cdots & F_{n,d} \end{bmatrix} \tag{19}$$

The search space's upper bound (ub) and lower bound (lb) are as follows:

$$ub = [ub_1, ub_2, ub_3, \cdots\cdots, ub_{n-1}, ub_n] \tag{20}$$

$$lb = [lb_1, lb_2, lb_3, \cdots\cdots, lb_{n-1}, lb_n] \tag{21}$$

3.1.2. The Moth's Location Updating

The logarithmic spiral function (S) that the moth flies according to is constructed as follows:

$$S(K_i, F_j) = d_i \times e^{at} \times cos(2\pi t) + F_j \tag{22}$$

where the symbol K_i indicates the i-th moth and designates a spiral function, and F_j signifies the location of the j-th flame. The constant a represents the value required to preserve the shape of the logarithm spiral. The distance between the j-th flame and the i-th moth is denoted as d_i. The random integer t is the distance parameters. The computation of the value of d_i is performed by employing Equation (20), defined as a value between -1 and +1.

$$d_i = |F_j - K_i| \tag{23}$$

The variable Ki represents the position of the i-th flame, F_j represents the position of the j-th moth, and the distance between the j-th flame and the i-th moth is represented by i and is updated by the following:

$$flame\ number = round\left((N - L) \times \frac{N-1}{T}\right) \tag{24}$$

where N indicates the upper limit of flames, T marks the upper limit of iterations, and L represents the current number of iterations. The adjustment of the position of each moth in relation to a flame is determined by the following equation.

3.2. Modified Moth Flame Optimizer

The MMFO is an enhanced version of the moth flame optimization (MFO) algorithm, where the movement of moths is based on the Archimedean spiral rather than the logarithmic spiral used in the standard MFO. The flight paths of the moths toward flames follow a spiral trajectory, providing better exploration and exploitation of the search space.

The position update formula for the MMFO using the Archimedean spiral is mathematically expressed as follows:

$$M_i^{t+1} = F_i + D.e^{b.l} \times cos(2\pi l) \tag{25}$$

where M_i^{t+1} is the updated position of the moth iii at iteration $t + 1$, F_i is the position of the flame i (the best solution found so far), D is the distance between the moth and the flame, b controls the shape of the spiral, and l is a random number in the range $[-1,1]$.

This Archimedean spiral enables moths to perform adaptive movements, which ensures a balanced exploration of the search space early in the optimization process and a more focused exploitation near the optimal solutions in later stages.

Archimedean Spiral Motion

The core idea of the MMFO is to update the position of each moth based on the Archimedean spiral toward a flame. This spiral is given by the following:

$$M_i^{t+1} = F_i + D.l \tag{26}$$

Here, $D = \left|M_i^{t+1} - F_i\right|$ is the Euclidean distance between the moth and the flame. The Archimedean spiral is described mathematically as follows:

$$S(\theta) = r(\theta).(cos\theta, sin\theta) \tag{27}$$

where $r(\theta) = a + b.\theta)$ defines the radius of the spiral as a function of the angle θ, and a and b are constants controlling the growth of the spiral. For the MMFO, this translates to the following:

$$M_i^{t+1} = F_i + (a + b.\theta).(cos\theta, sin\theta) \tag{28}$$

where a controls the initial radius of the spiral, b defines how fast the spiral expands or contracts, and θ is a random value determining the angle of the spiral. Also, the coordinate for the Archimedean spiral could be found in [34,35].

This equation ensures that moths follow a spiral trajectory toward the flames, where they explore the search space in wide arcs initially (exploration) and tighten their paths as they converge toward the best solutions (exploitation). The pseudocode summary and graphical abstract of the proposed MMFO is given in Algorithm 1 and Figure 1.

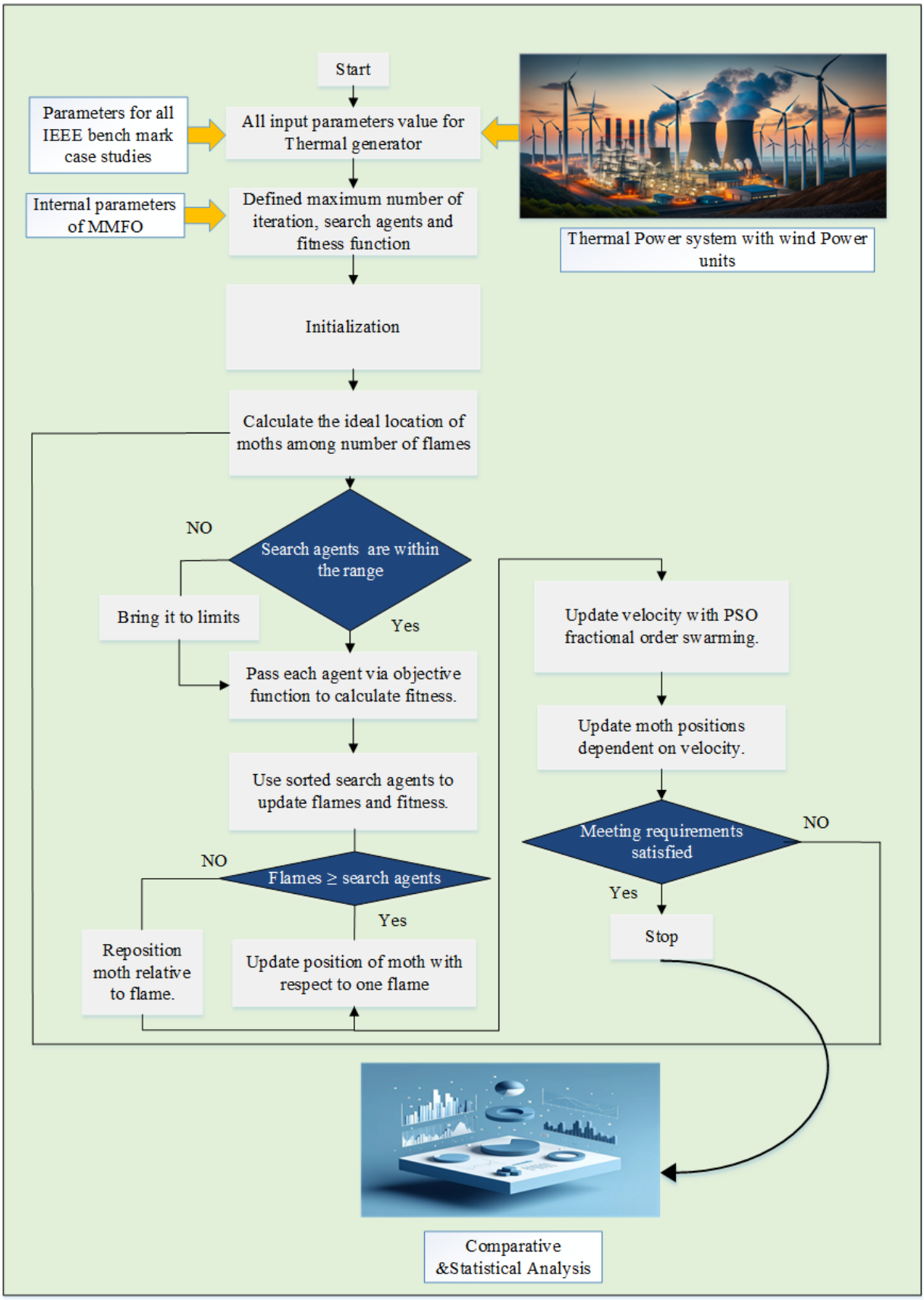

Figure 1. Graphical abstract of the proposed methodology.

Algorithm 1: Pseudocode of MMFO

1. Initialize parameters:

   Number of moths (N);
   Maximum number of iterations (MaxIter);
   Search space bounds (LB, UB);
   Moths' positions (M) randomly within the search space;
   Number of flames (F), initially equal to N.

2. Initialize flames (best solutions):

   Set the initial positions of flames (F) as the top N moths' positions.

3. Evaluate the fitness of all moths:

   For each moth Mi, evaluate the fitness using the objective function.

4. Sort moths based on fitness:

   Rank moths from best to worst based on fitness values.
   The best moths are selected as flames (F).

5. Loop through iterations (t = 1 to MaxIter):
   a. Update number of flames dynamically:
      Reduce the number of flames as iterations progress.
      Flame_no = round ($N - t \times (N - 1)$/MaxIter)
   b. For each moth Mi (i = 1 to N):
      i. Select the corresponding flame F_i:
         If $i \leq$ Flame_no, select the i-th flame;
         If $i >$ Flame_no, select the last flame.
      ii. Calculate distance between the moth and the flame: $D = |F_i - M_i|$
      iii. Update moth position using Archimedean spiral:
         $M_i{}^{t+1} = F_i + D.l$
         where l is a random number in the range $[-1, 1]$, determining the spiral movement's direction and distance.
      iv. Ensure the updated moth position is within search bounds (LB, UB).
   c. Evaluate the fitness of updated moths:
      For each updated moth Mi, calculate its fitness using the objective function.
   d. Sort moths based on their updated fitness:
      Rank all moths based on fitness values.
   e. Update flames:
      Select the top Flame_no moths as the new flames for the next iteration.
   f. Check stopping criteria:
      If the maximum number of iterations is reached or the convergence condition is met, exit the loop.

6. Return the best flame (optimal solution) as the result.

4. Results and Discussion

The effectiveness of the proposed MMFO approach in solving the constraint optimization problem is assessed by initially applying it on a standard benchmark function. The most effective way for evaluating optimization techniques is to employ to standard unimodal and multimodal benchmark functions. The optimizer with the lowest error is regarded as a good optimizer [30,31]. For a fair comparison of performances of the proposed MMFO and other competing algorithms in solving the benchmark, common and default settings for all and individual algorithms are shown in Table 1.

Table 1. Common and default settings for all algorithms.

Common Setting			Default Setting
Algorithm	**Population Size**	**Number of Iterations**	
PSO	30	1000	Inertia weight = 0.7, cognitive C_1 = 2, Social (C_2) = 2
GSA	30	1000	Gravitational constant (G) = 1
BA	30	1000	Loudness (A) = 0.5, pulse rate = 0.5
MFO	30	1000	Spiral function parameter (b) = 1
MMFO	30	1000	b = 1 + 0.5 × (1 − Iteration/Max_iteration);

In order to evaluate different optimization methods across different contexts, this paper uses a complete set of 11 benchmark functions. Unimodal functions are the first seven functions (F1–F7), whereas multimodal functions are the last four functions (F8–F11). All these benchmark functions have been taken from [28]. The MMFO achieves an optimum result in all different test scenarios. The results are tabulated in Table 2 which shows the performance of MMFO in terms of average fitness value over 100 independent runs with other state-of-the-art solvers, and it has been observed that the MMFO surpasses other optimization techniques in terms of average fitness value. To further demonstrate the superiority of our proposed optimizer, it has been also applied to a set of 10 benchmark functions consisting of different multimodal multi-objective optimization functions. The mathematical formulation and function details could be found in reference [36]. From Table 3, it has been realized that the MMFO outperforms the conventional MFO in terms of best, median, mean, and worst value and optimizes it up to optimum values. The results shown in Table 4 present statistically significant differences between MMFO and MFO in all metrics, with *p*-values below 0.05 using the Wilcoxon test. This indicates that MMFO exhibits a distinct optimization performance compared to MFO, suggesting that the modifications in MMFO have a substantial impact on the optimization outcomes. The consistent differences across metrics highlight the different behaviors of these two methods. In Table 4, it has been further concluded that the null hypothesis (H0) is rejected in all scenarios which indicates that our proposed MMFO differed significantly and outperformed its counterpart MFO.

In order to further validate the performance of the MMFO approach, it is first applied on the conventional ELD problem, which entails minimizing fuel cost. This assessment is carried out utilizing two practical benchmark IEEE testing systems. The subsequent content is presented as follows.

Case study 1 examines a small test system including three thermal units, each supporting a load requirement of 850 MW. The second case study focuses on a medium-sized test system consisting of 13 thermal generating units having a load demand of 1800 MW.

After validating the performance to solve the traditional ELD problem, the suggested technique minimizes fuel cost and emission by taking into consideration VPLEs, transmission line loss generator limitations of a standard IEEE benchmark system consisting of six power units for emission, and forty power units for wind power.

Table 2. MMFO comparison with other solvers for unimodal and multimodal benchmark functions.

Functions	Dim	MFO [28]		PSO [28]		GSA [28]		BA [28]		MMFO	
		Mean	STD	Mean	STD	Mean	STD	Mean	STD	Mean	STD
$F_1(x) = \sum_{i=1}^{n} x_i^2$	100	0.000117	0.00015	1.32115	1.15388	608.232	464.654	20792.4	5892.40	0.0039	0.0031
$F_2(x) = \sum_{i=1}^{n} \lvert x_i \rvert + \prod_{i=1}^{n} \lvert x_i \rvert$	100	0.000639	0.000877	7.71556	4.13212	22.7526	3.36513	89.785	41.9577	0.0040	0.0014
$F_3(x) = \sum_{i=1}^{n} \left(\sum_{j-1}^{i} x_j \right)^2$	100	696.730	188.527	736.393	361.781	135,760	48,652.6	62,481.3	29,769.1	1.4061×10^3	1.6103×10^3
$F_4(x) = \max_i \{\lvert x_i \rvert, 1 \leqslant i \leqslant n\}$	100	70.6864	5.27505	12.9728	2.63443	78.7819	2.81410	49.7432	10.14363	31.6315	10.5376
$F_5(x) = \sum_{i=1}^{n-1} \left[100\left(x_{i+1} - x_i^2\right)^2 + \left(x_i - 1\right)^2 \right]$	100	139.148	120.260	77,360.83	51,156.15	741.003	781.2393	199,512	125,238	83.1924	109.3115
$F_6(x) = \sum_{i=1}^{n} \left([x_i + 0.5] \right)^2$	100	0.00011	9.87×10^{-5}	286.651	107.079	3080.96	898.635	17,053.4	4917.56	0.0037	0.0027
$F_7(x) = \sum_{i=1}^{n} i x_i^4 + \text{random}[0, 1)$	100	0.091155	0.04642	1.037316	0.310315	0.112975	0.037607	6.045055	3.045277	0.0211	0.0064
$F_8(x) = \sum_{i=1}^{n} -x_i \sin\left(\sqrt{\lvert x_i \rvert}\right)$	100	8496.78	725.8737	−3571	430.7989	−2352.32	382.167	65,535	0	-9.4023×10^3	585.8782
$F_9(x) = \sum_{i=1}^{n} \left[x_i^2 - 10\cos(2\pi x_i) + 10 \right]$	100	84.600	16.1665	124.29	14.2509	31.0001	13.6605	96.2152	19.5875	74.9637	22.3468
$F_{10}(x) = -20\exp\left(-0.2\sqrt{\frac{1}{n}\sum_{i=1}^{n} x_i^2} \right) - \exp\left(\frac{1}{n}\sum_{i=1}^{n} \cos(2\pi x_i) \right) + 20 + e$	100	1.2603	0.72956	9.1679	1.56898	3.74098	0.17126	15.9460	0.77495	0.0958	0.4038
$F_{11}(x) = \frac{1}{4000}\sum_{i=1}^{n} x_i^2 - \prod_{i=1}^{n} \cos\left(\frac{x_i}{\sqrt{i}} \right) + 1$	100	0.0190	0.02173	12.418	4.16583	0.04978	0.04978	220.281	54.7066	0.0165	0.0143

Table 3. MMFO vs. MFO comparison for CEC2020 benchmark functions.

Function	Best		Median		Mean		Std		Worst	
	MMFO	**MFO**	**MMFO**	**MFO**	**MMFO**	**MFO**	**MMFO**	**MFO**	**MMFO**	**MFO**
F1	7.5000×10^{-1}	7.5605×10^{-1}	7.5000×10^{-1}	7.8610×10^{-1}	7.5004×10^{-1}	8.0100×10^{-1}	4.9873×10^{-4}	2.9151×10^{-3}	8.0952×10^{-1}	1.0502×10^{0}
F2	7.5000×10^{-1}	1.4078×10^{0}	7.5000×10^{-1}	1.4673×10^{0}	7.5251×10^{-1}	1.5807×10^{0}	1.1347×10^{-2}	2.6191×10^{-3}	1.9372×10^{0}	3.2955×10^{0}
F3	1.0000×10^{0}	1.0789×10^{0}	1.0000×10^{0}	1.0975×10^{0}	1.0002×10^{0}	1.1002×10^{0}	1.0677×10^{-3}	5.8074×10^{-5}	1.1315×10^{0}	1.1488×10^{0}
F4	7.5000×10^{-1}	1.5865×10^{0}	7.5000×10^{-1}	1.6938×10^{0}	7.5008×10^{-1}	1.7240×10^{0}	9.0085×10^{-4}	3.3394×10^{-3}	8.4823×10^{-1}	2.1179×10^{0}
F5	1.7559×10^{0}	7.4318×10^{-1}	1.7559×10^{0}	7.6418×10^{-1}	1.7560×10^{0}	7.6312×10^{-1}	4.5372×10^{-4}	1.4216×10^{-4}	1.8116×10^{0}	7.8235×10^{-1}
F6	1.0000×10^{0}	4.3480×10^{-4}	1.0000×10^{0}	2.2378×10^{-1}	1.0003×10^{0}	2.8438×10^{-1}	2.6533×10^{-3}	2.4468×10^{-3}	1.2731×10^{0}	8.6231×10^{-1}
F7	1.3603×10^{0}	1.8459×10^{0}	1.3603×10^{0}	2.0237×10^{0}	1.3607×10^{0}	2.0365×10^{0}	5.0828×10^{-3}	2.6639×10^{-4}	2.0788×10^{0}	2.4668×10^{0}
F8	2.0373×10^{0}	4.4031×10^{0}	2.0373×10^{0}	4.5035×10^{0}	2.0375×10^{0}	4.5165×10^{0}	2.7515×10^{-3}	1.3499×10^{-4}	2.4898×10^{0}	4.7865×10^{0}
F9	9.5950×10^{-1}	1.2183×10^{0}	9.5950×10^{-1}	1.2426×10^{0}	9.5975×10^{-1}	1.2480×10^{0}	2.5713×10^{-3}	6.9523×10^{-5}	1.2761×10^{0}	1.3536×10^{0}
F10	2.9160×10^{0}	1.3471×10^{1}	2.9160×10^{0}	1.3637×10^{1}	2.9161×10^{0}	1.3695×10^{1}	2.8887×10^{-4}	5.7093×10^{-4}	2.9544×10^{0}	1.4400×10^{1}

Table 4. Statistical comparison of MMFO and MFO performance using Wilcoxon signed-rank test.

Test Metric	*p*-Value	Test Statistic (W)	Conclusion (Reject H0)
Best value	0.0001	116866.0000	Yes
Median value	0.0000	116867.0000	Yes
Mean value	0.0001	116884.0000	Yes
Std	0.0000	423354.0000	Yes
Worst value	0.0000	129714.0000	Yes

4.1. Case 1. Three Thermal Generating Units with a Load Demand of 850 MW

The purpose of this case study is to assess the performance of the proposed MMFO and MFO with a load demand of 850 MW using a three-unit producing system, taking into account the valve-point loading impact. The parameters for fuel cost and the upper and lower limits for generators have been sourced from references [17,33,37–42]. The findings derived from the use of MMFO and MFO are presented in Table 5, alongside the findings documented in the existing literature. Table 6 illustrates the distribution of powers among several generators in response to a specified load demand of 850 MW. The suggested MMFO algorithm demonstrates superior performance, achieving a total cost of 8194.48008 USD/h, in comparison to MFO and other state-of-the-art algorithms.

Table 5. Optimum results for case 1 with other optimization techniques.

Algorithm	P1 (MW)	P1 (MW)	P1 (MW)	PG (MW)	Cost (USD/h)
GSA [39]	300.210	149.795	399.995	850	8234.1
PSO-SQP [38]	300.3	400	149.7	850	8234.1
PSO [38]	300.3	400	149.7	850	8234.1
GA [38]	398.7	399.6	50.1	848.4	8222.1
GA-PS-SQP [38]	300.30	400	149.70	850	8234.10
QOPO [43]	300.25	400	149.75	850	8234.07
MFO	358.0935	365.7145	126.192	850	8198.2314
MMFO	396.769	328.4747	124.7563	850	8194.4800

Table 6. Comparison of total fuel cost with up-to-date algorithms for case 1.

Method	Minimum Cost (USD/h)
GWO [13]	8253.11
GA [37]	8234.419
EP [37]	8234.1357
SA [37]	8234.1355
GA-PS-SQP [38]	8234.1
CPSO-SQP [41]	8234.07
NDS [44]	8234.07
MFEP [40]	8234.08
NSS [37]	8234.08
CPSO [41]	8234.07
GSA[39]	8234.1
iBA [42]	8234.07
GAB [40]	8234.08
QOPO [43]	8234.07
MFO	8198.23141
MMFO	8194.48008

Moreover, the findings are succinctly presented in Table 6 and juxtaposed with alternative comparison methodologies proposed in the existing literature. The proposed method yields superior outcomes compared to previous procedures. It has been seen that the proposed method achieved a superior solution and minimized the overall fuel cost to the optimal level, demonstrating the superiority of the suggested technique over other state-of-the-art algorithms in terms of total net gain in cost (USD/h). Figure 2 displays the convergence characteristic graph of MMFO vs. MFO, illustrating a more rapid convergence and the achievement of the lowest fuel cost within a reduced number of iterations as compared to MFO. Figure 3 shows the statistical analysis of MMFO vs MFO using cumulative distribution function (CDF), histograms, boxplot and fitness propagation obtained during the course of simulation

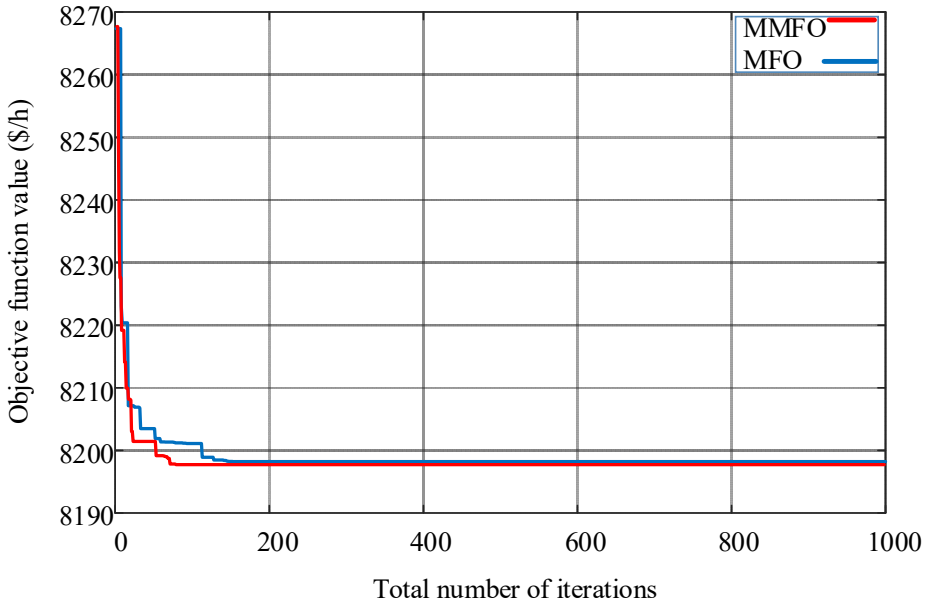

Figure 2. MMFO vs. MFO convergence characteristics curve for case 1.

4.2. Case 2. Thirteen Thermal Generating Units with 1800 MW Load Demands

This case study examines the efficacy of the suggested MMFO with load requirements of 1800 MW using the system of 13 generating units, taking into account the valve-point loading effect. The parameters for fuel cost and the upper and lower limits for generators have been sourced from references [8,17,38,40,43,45,46]. The outcomes derived using MMFO and MFO are presented in Table 7 for load demands of 1800 MW, in addition to the findings reported in the literature. Table 7 depicts the distribution of power among various generators in response to load demands of 1800 MW. The suggested MMFO demonstrates superior outcomes, with a total expenditure of 17,960.14253 USD/h. The data presented in Table 8 clearly demonstrate that the suggested method outperforms other strategies, including conventional Fast EP (FEP), EP (CEP), MFEP, enhanced FEP (IFEP), and PSO. With the expansion of the system to 13 units, the suggested technique has demonstrated a significant cost reduction of at least USD per hour in comparison to the Fast EP (FEP), MFEP, and PSO techniques for a load requirement of 1800 MW. The aforementioned results demonstrate the efficacy of the suggested MMFO approach. Figure 4 indicates that the MMFO and MFO convergence characteristic allows it to reach the global optimal solution with fewer iterations. When compared to other methods discussed in the relevant literature, the suggested MMFO has shown to be more effective. Optimal fuel cost and enhanced convergence rate have improved the solution's overall quality. Figure 5 shows the complete statistical analysis of the proposed MMFO VS MFO consisting of CDF, histogram, boxplot and fitness propagation demonstrating the reliability consistency of MMFO over MFO.

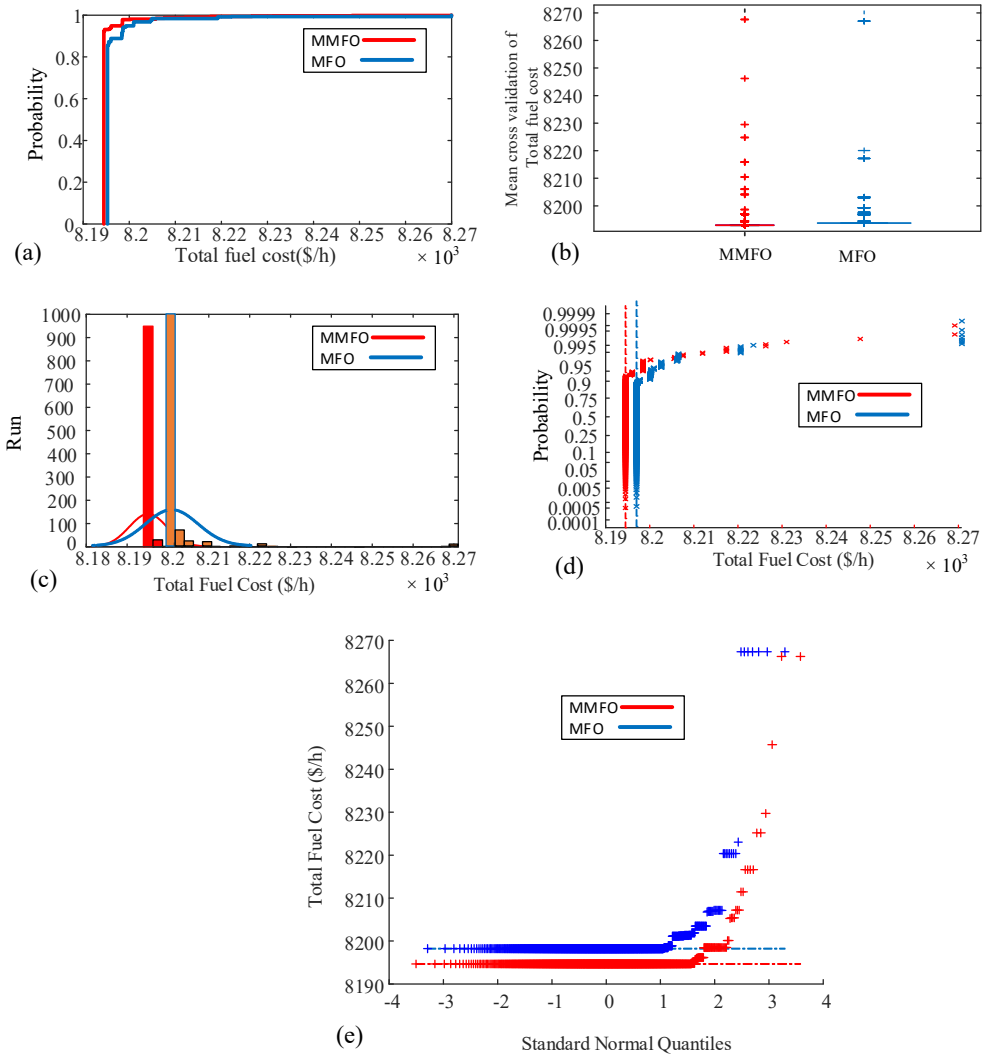

Figure 3. MMFO vs. MFO comparison during total fuel cost minimization for 3 thermal generating units: (**a**) CDF, (**b**) boxplot illustration, (**c**) histogram, (**d**) probability plot for normal distribution, and (**e**) quantile–quantile plot.

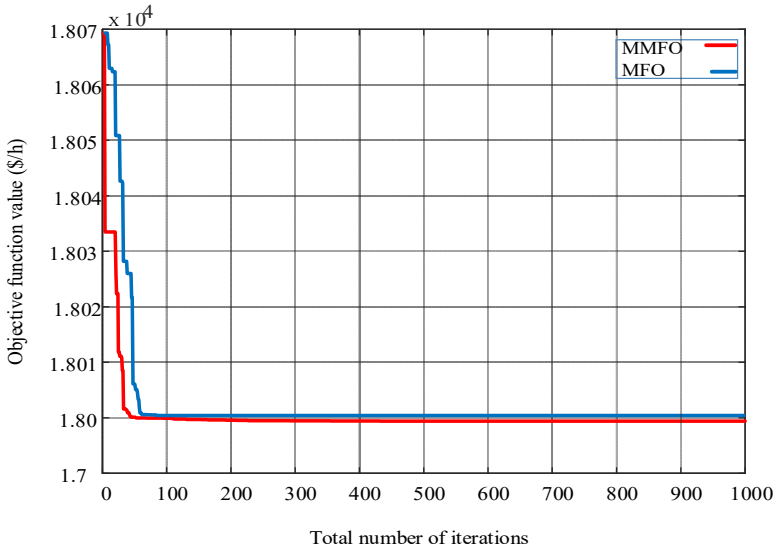

Figure 4. Convergence characteristic of MMFO vs. MFO for 13-unit system.

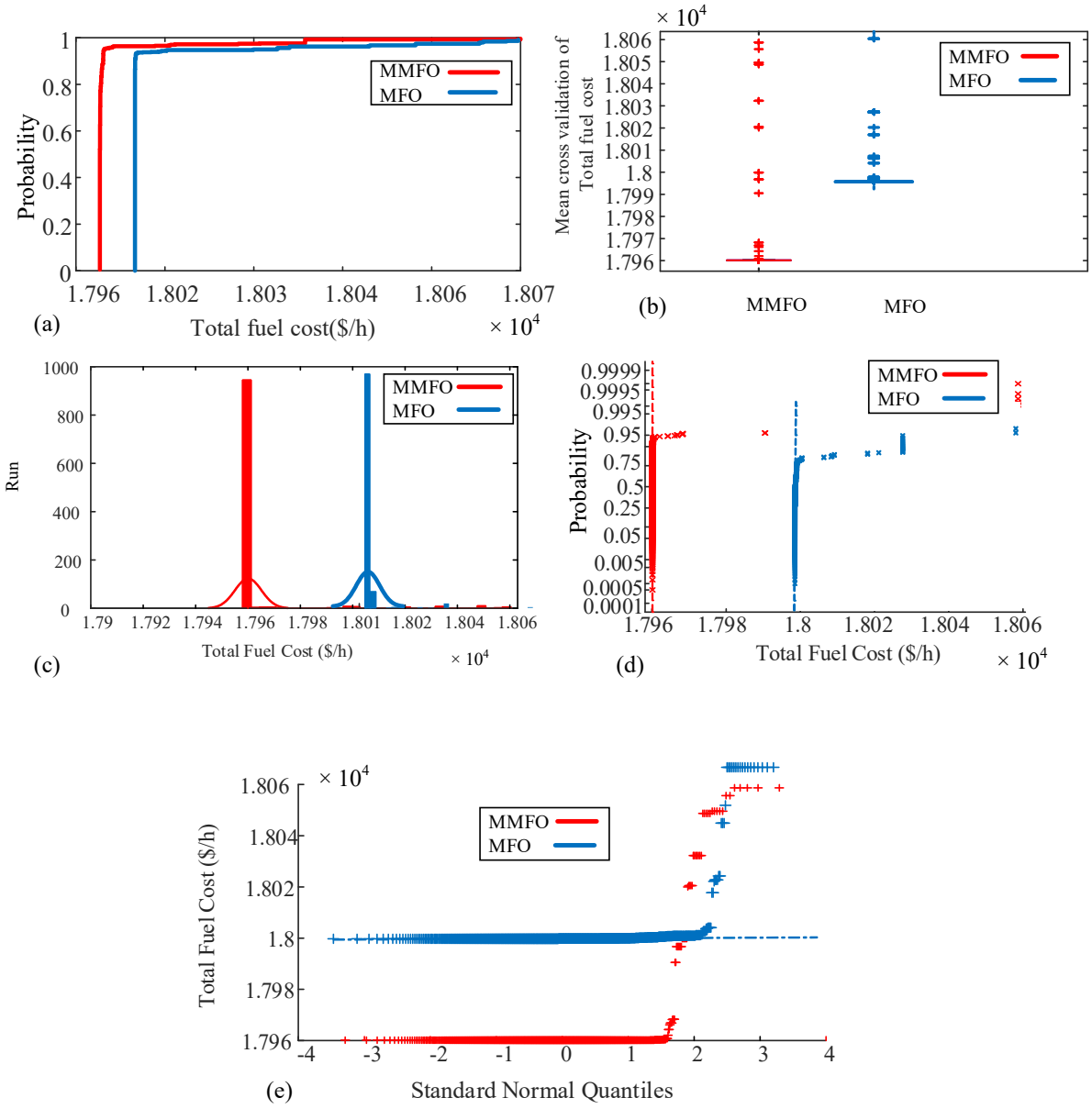

Figure 5. MMFO vs. MFO comparison during total fuel cost minimization for 13 thermal generating units: (**a**) CDF, (**b**) boxplot illustration, (**c**) histogram, (**d**) probability plot for normal distribution, and (**e**) quantile–quantile plot.

Table 7. Optimum power distribution for 13 generator units with other algorithms.

Unit	GWO [13]	NN-EPSO [13]	MFO	MMFO
1	807.1247	490	532.6321	481.7726
2	144.869	189	305.1329	194.1905
3	297.9434	214	89.01453	244.7307
4	60	160	117.7604	116.1982
5	60	90	117.7238	117.4941
6	60	120	122.1081	132.1647
7	60	103	60	77.94045

Table 7. *Cont.*

Unit	GWO [13]	NN-EPSO [13]	MFO	MMFO
8	60	88	99.69107	125.2659
9	60.0362	104	92.019	92.16435
10	40	13	40	40
11	40.0267	58	48.91808	43.26936
12	55	66	120	78.6438
13	55	55	55	56.16537
TG (MW)	1800	1750	1800	1800
Total Cost (USD/h)	18,051.11	18,442.59	18,008.89	17,960.14

Table 8. Comparison of total fuel cost with up-to-date algorithms for case 2.

Technique	Total Fuel Cost (USD/h)
MFEP [40]	18,028.09
FEP [40]	18,018.00
PSO [43]	18,030.72
CEP [40]	18,048.21
MFO	18,008.89
MMFO	17,960.14253

4.3. Case 3. Six Generating Units with 1000 MW Load Demand with Emission

A small test system has been used in this scenario to assess its efficacy in delivering a more efficient and precise solution for high load demand. The generator maximum and lowest limitations, emission coefficients, and fuel cost coefficients have been extracted from references [43,47–50]. Table 9 displays the optimal solutions obtained by MMFO, which includes the power generating output of each unit for the economic emission dispatch (EELD) problem. This study examines the outcomes obtained utilizing the scalar factor w. It has been noticed that when w is set to 0.5, the desired balance values are reached. In this situation, the EELD problem obtained with a weight (w) of 0.5, as shown in the table, has been selected for further investigation and comparison [4]. Table 10 presents a comparison of the solutions obtained by MMFO and other previously published approaches for minimizing fuel cost (FC) in ELD and minimizing emissions (E) in the economic emission issue. Based on the table, MMFO has produced lower results for the lowest fuel cost compared to other algorithms. The acquired findings are compared with nine distinct strategies that have been suggested in the literature and sourced from [43] The simulation results indicate that the suggested MMFO approach offers superior fuel cost compared to other strategies but with somewhat higher emissions compared to NGPSO. The emission level is significantly elevated owing to the significant reduction in fuel cost of 51,337.3323 USD/h, which is 15,201.0077 USD/h lower than NGPSO. In addition, the suggested MMFO approach has been shown to provide both the lowest fuel cost and the lowest pollution cost when compared to other strategies. The graph in Figure 6 illustrates the convergence characteristic of total fuel cost when using various scaling factors. It reveals that the convergence is rapid and achieves the optimal solution in a reduced number of iterations. Thus, it can be said that the suggested MMFO offers a superior and better compromised solution.

Table 9. Optimum power allocation among 6 units for different values of w.

w	P1	P2	P3	P4	P5	P6	Total Load	Fuel Cost (USD/h)	Emission (tons/h)
0	103.652	99.53047	154.1789	159.767	246.1043	236.7673	1000	52,009.8943	801.4391
0.1	103.652	99.53047	154.1789	159.767	246.1043	236.7673	1000	51,796.5424	807.0951
0.2	103.652	99.53047	154.1789	159.767	246.1043	236.7673	1000	51,812.7033	806.5594
0.3	103.652	99.53047	154.1789	159.767	246.1043	236.7673	1000	51,616.4886	813.7519
0.4	103.652	99.53047	154.1789	159.767	246.1043	236.7673	1000	51,347.5181	824.8128
0.5	103.652	99.53047	154.1789	159.767	246.1043	236.7673	1000	51,337.3323	824.4148
0.6	103.652	99.53047	154.1789	159.767	246.1043	236.7673	1000	51,048.3607	842.7160
0.7	103.652	99.53047	154.1789	159.767	246.1043	236.7673	1000	51,023.9795	845.2482
0.8	103.652	99.53047	154.1789	159.767	246.1043	236.7673	1000	50,824.5949	862.3027
0.9	103.652	99.53047	154.1789	159.767	246.1043	236.7673	1000	50,508.2147	910.1253
1	103.652	99.53047	154.1789	159.767	246.1043	236.7673	1000	50,385.4867	986.7312

Table 10. Comparison of results of six-unit system with other algorithms.

Unit	1	2	3	4	5	6	C	E
QOTLBO	107.3101	121.497	206.501	206.5826	304.9838	304.6036	64,912	1281
TLBO	107.8651	121.5676	206.1771	205.1879	306.5555	304.1423	64,922	1281
MODE	108.6284	115.9456	206.7969	210	301.8884	308.4127	64,843	1286
PDE	107.3965	122.1418	206.7536	203.7047	308.1045	303.3797	64,920	1281
NSGA	113.1259	116.4488	217.4191	207.9492	304.6641	291.5969	64,962	1281
SPEA	104.1573	122.9807	214.9553	203.1387	316.0302	289.9396	64,884	1285
MOGA	108.9318	123.1808	205.1513	206.67	304.8553	302.6093	64,838.57	1285.49
OGHS	105.7331	119.0825	205.2976	204.7772	305.8042	308.9128	64,722.74	1281.349
NGPSO	144.0425	150	190.507	192.9285	284.9083	288.0456	66,538.34	1228.365
QOPO	82.83027	82.61994	197.7722	202.2269	317.4203	317.6234	61,197.88	1238.819
MMFO	103.652	99.53047	154.1789	159.767	246.1043	236.7673	51,337.3323	824.4148

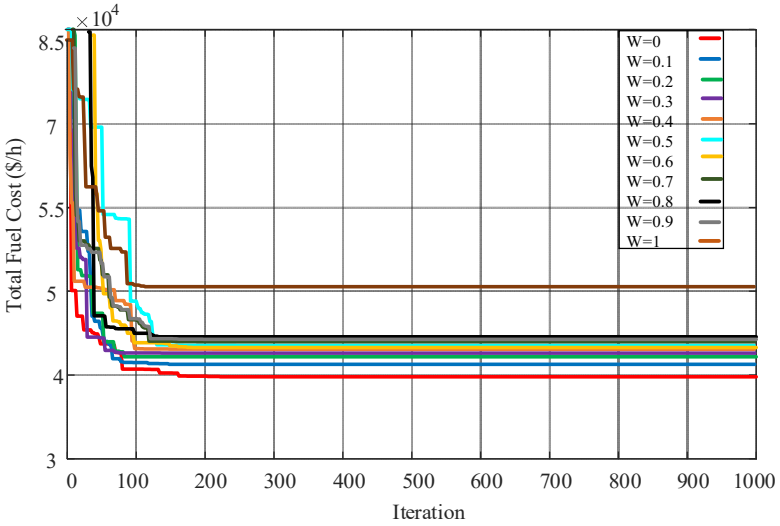

Figure 6. MMFO convergence graphs for IEEE six-generator system with different scaling.

4.4. Case 4. Thirty-Seven Thermal Generating Units and Three Wind Power Units with Demand of 10,500 MW

This scenario investigates a modified case study of ELD-VPLE, focusing on a total of 40 generators. Specifically, the analysis includes thirty-seven thermal power generating units and three units of wind power producing units, which are examined for the bi-objective function. The integration of ELD-VPLE with wind power is achieved by employing the system model formulation of Equation (3). Equation (5) is used to include the total cost of generation. The dataset containing information on thermal and wind power generating units has been sourced from references [27,45,46,51,52]. Table 11 depicts the distribution of power among various generators in response to load demands of 10,500 MW. Table 12 presents the optimal overall cost value in dollars per hour when compared to alternative algorithms. Furthermore, it has been shown that the suggested MMFO exhibits strong performance in the context of bi-objective functions, thereby reducing the overall fuel cost to an optimal level. Furthermore, it has significantly enhanced the overall quality of the solution in terms of achieving the most efficient fuel cost, faster convergence rate, and improved dependability. As shown in Figure 7, the minimum fitness value is obtained in a fewer number of iterations; furthermore, it has been observed that the convergence process is expedited, resulting in a shorter number of iterations to obtain the global optimum solution.

Table 11. Optimum power allocation for 40-unit test system (37 thermal and 3 wind power units).

Power Units	MFO	MMFO	Power Units	MFO	MMFO
1	114	112.2146	21	523.2265	534.9080
2	110.782043	85.7714	22	345.1678	519.7360
3	97.35768193	88.2117	23	523.2798	461.0149
4	179.853732	180.9641	24	550	532.9676
5	47	82.4790	25	523.2365	532.8027
6	140	139.9986	26	522.6056	541.2884
7	300	300	27	47	80.9368
8	300	289.7228	28	163.3979	112.6556
9	285.1041	288.4185	29	169.6291	126.9149
10	130	200.5044	30	190	158.8551
11	318.0878	289.2551	31	172.465	199.9890
12	94	243.7934	32	166.535	172.3346
13	216.8874	304.4608	33	90	90
14	484.0405941	390.7212	34	65.63347	86.84495
15	500	500	35	110	57.10207
16	500	353.3224	36	110	72.98398
17	500	313.0460	37	511.2403	500.4913
18	220	421.2108	38	18	19.85508
19	511.4687	495.8544	39	46	46.0001
20	550	518.3697	40	54	54
Total cost MFO 139,576.3965			Total cost MMFO 138,155.7853		

Table 12. Comparison of total fuel cost for 40-unit test system with wind power units.

Method	Minimum Cost (USD/h)
Best Compromise [51]	143,587.90
PSO [52]	139,000.03
DWTED2 [51]	154,993.00
PWTED2 [51]	156,878.97
EMA [27]	144,356.00
GAEPSO [27]	146,035.00
PSO [27]	142,068.00
COOT [52]	139,000.63
MFO	139,576.3965
MMFO	138,155.7853

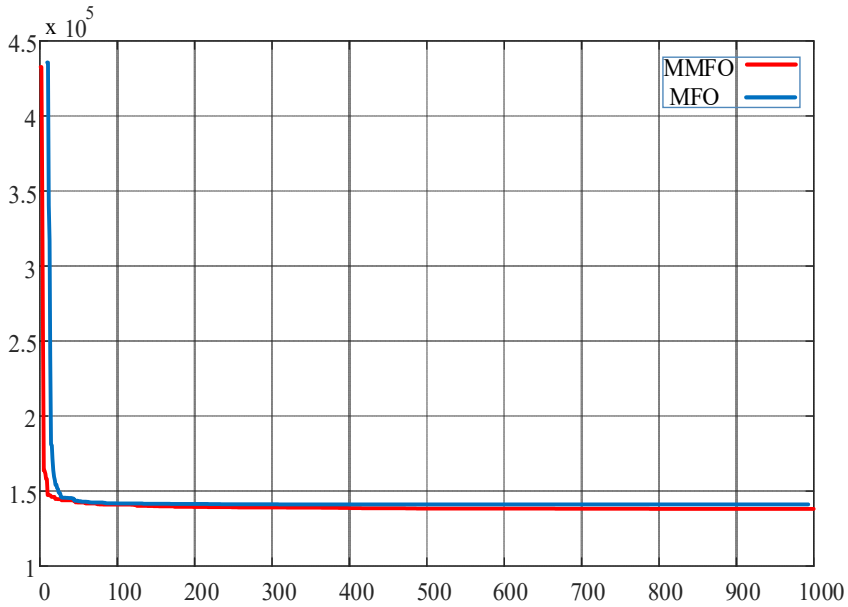

Figure 7. Convergence characteristic of MMFO vs. MFO for 40-unit system with wind power.

5. Comparative and Statistical Analysis

The proposed MMFO was applied to solve the ELD problem for the IEEE benchmark systems comprising three, six, eleven, and forty generating units, incorporating wind power effects. The results obtained by the proposed optimizer were aligned with and superior to those reported in references [13,27,37–46,51,52]. The MMFO successfully achieved optimal solutions for addressing the ELD problem while considering both emission constraints and wind power factors. The findings confirm that MMFO outperforms other optimization methods in solving this non-convex, non-linear, and complex optimization problem, offering a faster convergence rate. In comparison with methods cited in the literature, the MMFO demonstrated superior performance under similar boundary conditions and characteristics. Convergence graphs from the simulations across all case studies highlight MMFO's faster convergence and ability to find optimal solutions in fewer iterations. As evidenced in Tables 6, 8, 10, and 12, the proposed MMFO achieved a significant reduction in total fuel cost, demonstrating a clear advantage over state-of-the-art techniques. The results show that MMFO consistently improves solution quality and minimizes total cost to its optimal value. A comprehensive statistical analysis was conducted on the test systems to ensure the dependability, consistency, and stability of the proposed method. A total of 100 indepen-

dent simulations were performed, with the median outcome serving as a benchmark for determining the best solution. Figures 3, 5 and 8 provide a quantitative analysis using the empirical cumulative distribution function (CDF), histograms, boxplots, and fitness progressions in each independent run. Figures 3a, 5a, and 8a demonstrate that MMFO significantly increases the probability of finding the optimal solution compared to traditional MFO. Figures 3b, 5b and 8b reveal that MMFO consistently achieves a lower median of the final solution in 100 trials compared to MFO, while Figures 3c, 5c, and 8c show the histogram indicating minimal fitness after multiple trials. Moreover, Figures 3d, 5d and 8d reflect the probability distribution for normality, indicating that MMFO has a higher likelihood of solving the ELD and EELD problems more efficiently than conventional MFO. Finally, Figures 3e, 5e and 8e show that MMFO exhibits a favorable minimum fitness relative to the quantiles of the normal distribution. Based on these visual and graphical analyses, it is evident that incorporating the Archimedean spiral into the optimization framework significantly enhances MMFO's performance and serves as a robust mathematical tool for developing new variants of traditional optimization techniques.

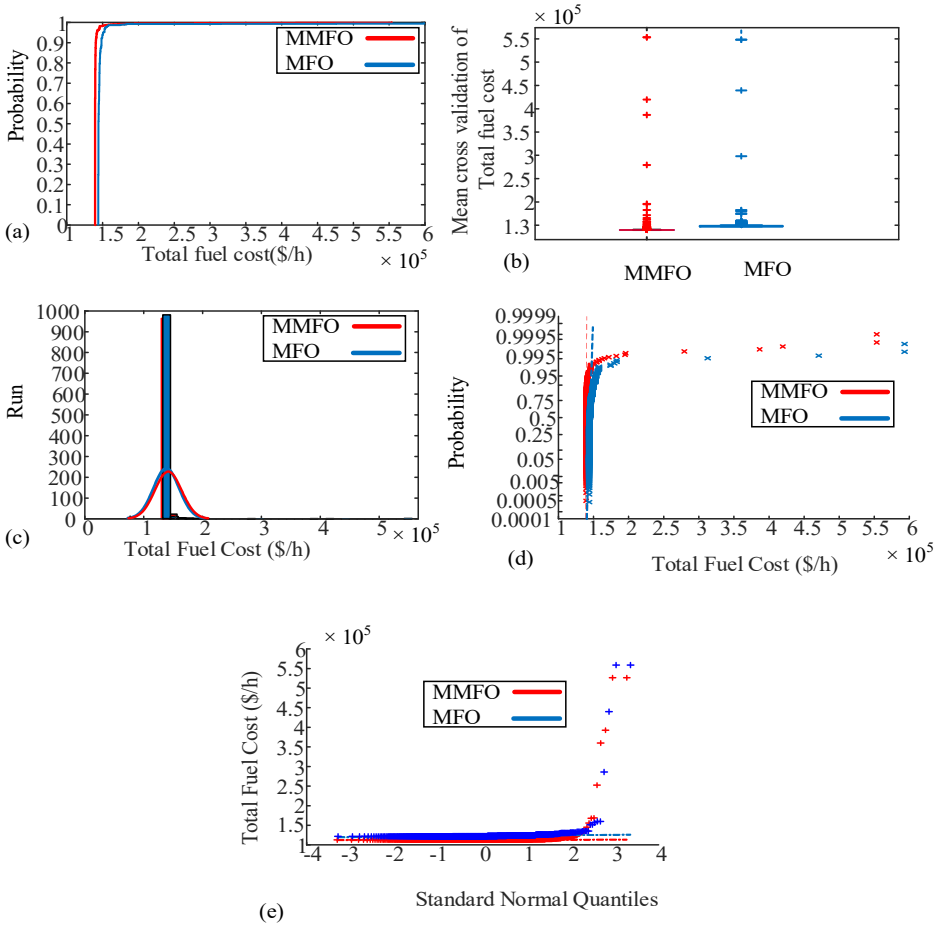

Figure 8. MMFO vs. MFO statistical analysis during total fuel cost minimization for 37 thermal generating units and 3 wind power: (**a**) CDF, (**b**) boxplot illustration, (**c**) histogram, (**d**) probability plot for normal distribution, and (**e**) quantile–quantile plot.

6. Conclusions

This study introduces a novel variant of the moth flame optimization algorithm, termed MMFO, designed to address the complex ELD and EELD problems, which are characterized by non-linearity, non-convexity, and non-smoothness. The proposed MMFO method is initially validated through its application to a wide range of generating units, from small systems with three units to large-scale systems with up to forty units, demonstrating its capability to deliver reliable and competitive solutions.

The effectiveness and performance of the MMFO approach are assessed across various scales, including small (three units and six units with emission), medium (thirteen units), and large (forty units) generating systems consisting of thirty-seven thermal and three wind power units. The evaluation considers fuel cost, emission cost, and wind power cost under different load demands and constraints. Comparative results highlight the efficacy of the proposed method in solving simple ELD problems, EELD and ELD with wind power scenarios, by achieving the lowest cost and emissions in power generation across all unit sizes in distinct case studies.

For case 1, the proposed MMFO reveals an improvement in percentages of 0.71% for GWO, 0.485% for GA, and 0.48% over EP, SA, GA-PS-SQP, NDS, MEEP, NSS, HCPSO, GSA, iBA, GAB, QOPO, and MFO in total fuel cost in dollars per hour, keeping in view it is a very small system. For case 2, the optimal setting determined by MMFO with MEEP, FEP, PSO, CEP, and MFO shows an improvement in percentages of 0.3768%, 0.3211%, 0.3914, 0.4879%, and 0.2706%, respectively, in dollars per hour.

For case 3, the MMFO again has superiority in net improvement in percentage over other state-of-the-art solvers in both fuel cost and emission. There were observed net improvements in percentages in fuel cost of 20.912%, 20.924%, 20.828%, 20.922%, 20.973%, 20.878%, 20.822%, 20.681%, 22.845%, and 16.112% with QOTLBO, TLBO, MODE, PDE, NSGA, SPEA, MOGA, OGHS, NGPSO, and QOPO, respectively, while in the case of emission reduction, there was an improvement of 35.64% with QOTLBO and TLBO, 35.893% with MODE, 35.64 with PDE and NSGA, and 35.84%, 35.867%, 35.860%, and 35.88% with SPEA, MOGA, OGHS, NGPSO, and QOPO, respectively.

For case 4 consisting of thirty-seven thermal units and three wind power units, a net improvement in percentage in total fuel cost was obtained that corresponds to 3.783%, 0.6073%, 10.863%, 11.934%, 4.295%, 2.753%, 0.6077%, and 1.017%.

Furthermore, the method's reliability, robustness, and consistency are confirmed through statistical analyses, including cumulative distribution function (CDF) plots, lowest objective function values, normal distribution probabilities, and histogram representations across independent runs. The results reveal that incorporating the Archimedean spiral within the MFO framework significantly enhances the optimizer's convergence speed. The obtained results provide strong evidence of MMFO's efficiency in discovering superior and optimal solutions for the EELD problem, establishing MMFO as a highly effective tool for combined economic and emission optimization as well as for the ELD problem with wind power. Additionally, the proposed approach requires less computational effort and demonstrates superior convergence properties, achieving optimal trade-offs more efficiently than alternative methods.

In the future, the proposed MMFO will be implemented for real-time load dispatch in smart grids for fuel costs and emission optimization with the integration of more complex constraints in real-time power dispatch.

Author Contributions: Conceptualization, H.A., A.W. and H.P.; methodology, H.A., A.W. and H.P.; writing—original draft, H.A. and A.W.; writing—review and editing, A.W. and H.P.; supervision, A.W.; funding acquisition, H.A. and A.W. All authors have read and agreed to the published version of the manuscript.

Funding: This article is derived from a research grant funded by the Research, Development, and Innovation Authority (RDIA)—Kingdom of Saudi Arabia—with grant number (13385-Tabuk-2023-UT-R-3-1-SE).

Data Availability Statement: The original contributions presented in the study are included in the article, further inquiries can be directed to the corresponding author.

Acknowledgments: The authors extend their appreciation to the Research, Development, and Innovation Authority (RDIA), Saudi Arabia, for funding this work through grant number (13385-Tabuk-2023-UT-R-3-1-SE).

Conflicts of Interest: The authors declare that there are no conflicts of interest.

References

1. Arul, R.; Ravi, G.; Velusami, S. An improved harmony search algorithm to solve economic load dispatch problems with generator constraints. *Electr. Eng.* **2014**, *96*, 55–63. [CrossRef]
2. Yu, J.; Kim, C.-H.; Rhee, S.-B. Clustering cuckoo search optimization for economic load dispatch problem. *Neural Comput. Appl.* **2020**, *32*, 16951–16969. [CrossRef]
3. Walters, D.C.; Sheble, G.B. Genetic algorithm solution of economic dispatch with valve point loading. *IEEE Trans. Power Syst.* **1993**, *8*, 1325–1332. [CrossRef]
4. Ismaeel, A.A.; Houssein, E.H.; Khafaga, D.S.; Abdullah Aldakheel, E.; AbdElrazek, A.S.; Said, M. Performance of osprey optimization algorithm for solving economic load dispatch problem. *Mathematics* **2023**, *11*, 4107. [CrossRef]
5. Ramalingam, R.; Karunanidy, D.; Alshamrani, S.S.; Rashid, M.; Mathumohan, S.; Dumka, A. Oppositional Pigeon-Inspired Optimizer for Solving the Non-Convex Economic Load Dispatch Problem in Power Systems. *Mathematics* **2022**, *10*, 3315. [CrossRef]
6. Said, M.; El-Rifaie, A.M.; Tolba, M.A.; Houssein, E.H.; Deb, S. An efficient chameleon swarm algorithm for economic load dispatch problem. *Mathematics* **2021**, *9*, 2770. [CrossRef]
7. Chen, K.; Zhu, Z.; Wang, J. Economic dispatch for smart buildings with load demand of high volatility based on quasi-quadratic online adaptive dynamic programming. *Mathematics* **2022**, *10*, 4701. [CrossRef]
8. Hsieh, Y.-Z.; Su, M.-C. A Q-learning-based swarm optimization algorithm for economic dispatch problem. *Neural Comput. Appl.* **2016**, *27*, 2333–2350. [CrossRef]
9. Jain, N.K.; Nangia, U.; Jain, A. PSO for Multiobjective Economic Load Dispatch (MELD) for Minimizing Generation Cost and Transmission Losses. *J. Inst. Eng. Ser. B* **2016**, *97*, 185–191. [CrossRef]
10. Jain, N.K.; Nangia, U.; Jain, J. Economic Load Dispatch Using Adaptive Social Acceleration Constant Based Particle Swarm Optimization. *J. Inst. Eng. Ser. B* **2018**, *99*, 431–439. [CrossRef]
11. Jayabarathi, T.; Bahl, P.; Ohri, H.; Yazdani, A.; Ramesh, V. A hybrid BFA-PSO algorithm for economic dispatch with valve-point effects. *Front. Energy* **2012**, *6*, 155–163. [CrossRef]
12. Jayabarathi, T.; Yazdani, A.; Ramesh, V. Application of the invasive weed optimization algorithm to economic dispatch problems. *Front. Energy* **2012**, *6*, 255–259. [CrossRef]
13. Kamboj, V.K.; Bath, S.K.; Dhillon, J.S. Solution of non-convex economic load dispatch problem using Grey Wolf Optimizer. *Neural Comput. Appl.* **2016**, *27*, 1301–1316. [CrossRef]
14. Kamboj, V.K.; Bhadoria, A.; Bath, S.K. Solution of non-convex economic load dispatch problem for small-scale power systems using ant lion optimizer. *Neural Comput. Appl.* **2016**, *28*, 2181–2192. [CrossRef]
15. Labbi, Y.; Ben Attous, D. A hybrid particle swarm optimization and pattern search method to solve the economic load dispatch problem. *Int. J. Syst. Assur. Eng. Manag.* **2014**, *5*, 435–443. [CrossRef]
16. Labbi, Y.; Ben Attous, D. A Hybrid Big Bang–Big Crunch optimization algorithm for solving the different economic load dispatch problems. *Int. J. Syst. Assur. Eng. Manag.* **2017**, *8*, 275–286. [CrossRef]
17. Labbi, Y.; Ben Attous, D.; Mahdad, B. Artificial bee colony optimization for economic dispatch with valve point effect. *Front. Energy* **2017**, *8*, 449–458. [CrossRef]
18. Mahdad, B.; Srairi, K. Solving practical economic dispatch using hybrid GA–DE–PS method. *Int. J. Syst. Assur. Eng. Manag.* **2014**, *5*, 391–398. [CrossRef]
19. Murali, K.; Jayabarathi, T. Solution to economic dispatch problem with valve-point loading effect by using catfish PSO algorithm. *Front. Energy* **2014**, *8*, 290–296. [CrossRef]
20. Nascimento, M.H.R.; Nunes, M.V.A.; Rodríguez, J.L.M.; Leite, J.C. A new solution to the economical load dispatch of power plants and optimization using differential evolution. *Electr. Eng.* **2017**, *99*, 561–571. [CrossRef]
21. Pattanaik, J.K.; Basu, M.; Dash, D.P. Dynamic economic dispatch: A comparative study for differential evolution, particle swarm optimization, evolutionary programming, genetic algorithm, and simulated annealing. *J. Electr. Syst. Inf. Technol.* **2019**, *6*, 1. [CrossRef]
22. Prakash, T.; Singh, V.P.; Singh, S.P.; Mohanty, S.R. Economic load dispatch problem: Quasi-oppositional self-learning TLBO algorithm. *Energy Syst.* **2018**, *9*, 415–438. [CrossRef]
23. Yu, X.; Yu, X.; Lu, Y.; Sheng, J. Economic and emission dispatch using ensemble multi-objective differential evolution algorithm. *Sustainability* **2018**, *10*, 418. [CrossRef]
24. Jiang, S.; Ji, Z.; Wang, Y. A novel gravitational acceleration enhanced particle swarm optimization algorithm for wind–thermal economic emission dispatch problem considering wind power availability. *Int. J. Electr. Power Energy Syst.* **2015**, *73*, 1035–1050. [CrossRef]
25. Pandit, M.; Chaudhary, V.; Dubey, H.M.; Panigrahi, B. Multi-period wind integrated optimal dispatch using series PSO-DE with time-varying Gaussian membership function based fuzzy selection. *Int. J. Electr. Power Energy Syst.* **2015**, *73*, 259–272. [CrossRef]
26. Morshed, M.J.; Asgharpour, A. Hybrid imperialist competitive-sequential quadratic programming (HIC-SQP) algorithm for solving economic load dispatch with incorporating stochastic wind power: A comparative study on heuristic optimization techniques. *Energy Convers. Manag.* **2014**, *84*, 30–40. [CrossRef]
27. Hagh, M.T.; Kalajahi, S.M.S.; Ghorbani, N. Solution to economic emission dispatch problem including wind farms using Exchange Market Algorithm Method. *Appl. Soft Comput.* **2020**, *88*, 106044. [CrossRef]

28. Mirjalili, S. Moth-flame optimization algorithm: A novel nature-inspired heuristic paradigm. *Knowl. Based Syst.* **2015**, *89*, 228–249. [CrossRef]
29. Chang, C.C.W.; Ding, T.J.; Han, W.; Chai, C.C.; Yam, C.M.; Yian, H.C.; Xin, L.H. Moth flame optimization for the maximum power point tracking scheme of photovoltaic system under partial shading conditions. *Energy Rep.* **2023**, *9*, 374–379. [CrossRef]
30. Wadood, A.; Park, H. A Novel Application of Fractional Order Derivative Moth Flame Optimization Algorithm for Solving the Problem of Optimal Coordination of Directional Overcurrent Relays. *Fractal Fract.* **2024**, *8*, 251. [CrossRef]
31. Wadood, A.; Ahmed, E.; Rhee, S.B.; Sattar Khan, B. A Fractional-Order Archimedean Spiral Moth–Flame Optimization Strategy to Solve Optimal Power Flows. *Fractal Fract.* **2024**, *8*, 225. [CrossRef]
32. Nadimi-Shahraki, M.H.; Zamani, H.; Fatahi, A.; Mirjalili, S. MFO-SFR: An enhanced moth-flame optimization algorithm using an effective stagnation finding and replacing strategy. *Mathematics* **2023**, *11*, 862. [CrossRef]
33. Khan, B.S.; Raja, M.A.Z.; Qamar, A.; Chaudhary, N.I. Design of moth flame optimization heuristics for integrated power plant system containing stochastic wind. *Appl. Soft Comput.* **2021**, *104*, 107193. [CrossRef]
34. Hammer, Ø. *The Perfect Shape: Spiral Stories*; Springer: Berlin/Heidelberg, Germany, 2016.
35. Guo, M.; Wang, J.S.; Zhu, L.; Guo, S.S.; Xie, W. Improved ant lion optimizer based on spiral complex path searching patterns. *IEEE Access* **2020**, *8*, 22094–22126. [CrossRef]
36. Liang, J.J.; Qu, B.; Gong, D.W.; Yue, C. *Problem Definitions and Evaluation Criteria for the CEC 2019 Special Session on Multimodal Multiobjective Optimization*; Computational Intelligence Laboratory, Zhengzhou University: Zhengzhou, China, 2019; pp. 353–370.
37. Tsai, M.-T.; Gow, H.-J.; Lin, W.-M. A novel stochastic search method for the solution of economic dispatch problems with non-convex fuel cost functions. *Int. J. Electr. Power Energy Syst.* **2011**, *33*, 1070–1076. [CrossRef]
38. Alsumait, J.S.; Sykulski, J.K.; Al-Othman, A.K. A hybrid GA–PS–SQP method to solve power system valve-point economic dispatch problems. *Appl. Energy* **2010**, *87*, 1773–1781. [CrossRef]
39. Duman, S.; Güvenç, U.; Yörükeren, N. Gravitational search algorithm for economic dispatch with valve-point effects. *Int. Rev. Electr. Eng.* **2010**, *5*, 2890–2895.
40. Sinha, N.; Chakrabarti, R.; Chattopadhyay, P.K. Evolutionary programming techniques for economic load dispatch. *IEEE Trans. Evol. Comput.* **2003**, *7*, 83–94. [CrossRef]
41. Cai, J.; Li, Q.; Li, L.; Peng, H.; Yang, Y. A hybrid CPSO–SQP method for economic dispatch considering the valve-point effects. *Energy Convers. Manag.* **2012**, *53*, 175–181. [CrossRef]
42. Al-Betar, M.A.; Awadallah, M.A. Island bat algorithm for optimization. *Expert Syst. Appl.* **2018**, *107*, 126–145. [CrossRef]
43. Basetti, V.; Rangarajan, S.S.; Shiva, C.K.; Pulluri, H.; Kumar, R.; Collins, R.E.; Senjyu, T. Economic emission load dispatch problem with valve-point loading using a novel quasi-oppositional-based political optimizer. *Electronics* **2021**, *10*, 2596. [CrossRef]
44. Lin, W.-M.; Gow, H.-J.; Tsai, M.-T. Combining of Direct Search and Signal-to-Noise Ratio for economic dispatch optimization. *Energy Convers. Manag.* **2011**, *52*, 487–493. [CrossRef]
45. Wadood, A.; Sattar Khan, B.; Albalawi, H.; Alatwi, A.M. Design of the Novel Fractional Order Hybrid Whale Optimizer for Thermal Wind Power Generation Systems with Integration of Chaos Infused Wind Power. *Fractal Fract.* **2024**, *8*, 379. [CrossRef]
46. Wadood, A.; Khan, B.S.; Khurshaid, T.; Kim, K.C.; Rhee, S.B. Chaos-infused wind power integration in the grey wolf optimal paradigm for combine thermal-wind power plant systems. *Front. Energy Res.* **2024**, *12*, 1301700. [CrossRef]
47. Wadood, A.; Ghani, A. An application of Gorilla troops optimizer in solving the problem of economic load dispatch considering valve point loading effect. *Eng. Res. Express* **2024**, *6*, 015310.
48. Reddy, A.S.; Vaisakh, K. Shuffled differential evolution for large scale economic dispatch. *Electr. Power Syst. Res.* **2013**, *96*, 237–245. [CrossRef]
49. Zou, D.; Li, S.; Li, Z.; Kong, X. A new global particle swarm optimization for the economic emission dispatch with or without transmission losses. *Energy Convers. Manag.* **2017**, *139*, 45–70. [CrossRef]
50. Hassan, M.H.; Kamel, S.; Abualigah, L.; Eid, A. Development and application of slime mould algorithm for optimal economic emission dispatch. *Expert Syst. Appl.* **2021**, *182*, 115205. [CrossRef]
51. Azizipanah-Abarghooee, R.; Niknam, T.; Roosta, A.; Malekpour, A.R.; Zare, M. Probabilistic multiobjective wind-thermal economic emission dispatch based on point estimated method. *Energy* **2021**, *37*, 322–335. [CrossRef]
52. Khan, B.S.; Qamar, A.; Wadood, A.; Almuhanna, K.; Al-Shamma, A.A. Integrating economic load dispatch information into the blockchain smart contracts based on the fractional-order swarming optimizer. *Front. Energy Res.* **2024**, *12*, 1350076. [CrossRef]